

## An Efficient Photo Voltaic System for Onboard Ship Applications

Shashidhar Kasthala\*, Krishnapriya\*, Rajitha Saka\*\*

\*(Faculty of ECE, Indian Naval Academy, Ezhimala, Kerala-670310)

\*\* (Department of Electrical & Electronics, Gurunanak Institutions Technical Campus, Hyderabad)

### ABSTRACT

In this paper a high efficient photovoltaic system is proposed for onboard ship applications which convert the lower voltage obtained from solar modules to higher voltage required by the ship service loads. In a typical photovoltaic system only step-up /boost converter is used due to which the converter has to operate in extreme duty ratio, resulting in increase of switching losses and thus decreasing the overall efficiency. But in this paper the conventional boost converter is used with interleaved inductors and capacitors. The proposed system stores the energy in inductors and thus reduces the stress in the switches (Without allowing the total voltage to appear across the switch). The simulation is designed using MATLAB/Simulink with an Input voltage of 40-V to achieve a output voltage of 300-380 V. The developed simulation results are compared for output powers of 500W and 1kW

**Keywords** - Photovoltaic system, renewable energy sources, interleaved boost converter, voltage multiplier module.

### I. INTRODUCTION

Currently, the diesel engines, is considered has the most viable and reliable option for ship propulsion and auxillary power generation. But the complication with the extensive usage of this technology is emmission of gases like CO<sub>2</sub>, NO<sub>x</sub>, SO<sub>x</sub> and other organic chemicals. The shipping industry is estimated to produce 3% of global emmission of CO<sub>2</sub>, this includes the mechant ships, combat ship and cruise ships [7][8]. As a solution to this, extensive research is being carried out world wide in implementation of renewable energy sources for Ship propulsion and other Ship service loads. The renewable energy, primarily solar and wind energy sources can be considered as an alternative energy source for main propulsion and auxillary power requirements of a ship though there are some inherent limitations for these renewable energies due to their intermittent nature [4].

The electrical load on board ship can be classified into propulsion loads and service loads. With the present day solar technology and with the typical characteristics of propulsion drives, the solar energy has a primary source of energy may not be a feasibile option for medium or large ships but can be used for small size ships. For large size ships, the solar energy can be used to cater only the selected laods so as to mainatin the continuity of electrical supply. The solar energy on board ship can be connected to the vital loads viz. Combat systems, mobility systems, fire systems etc [1]. Fig. 1 shows a typical photovoltaic system catering the service loads of the ship which consists of a solar module, a step-

up converter, a controller, a battery set, and an inverter.

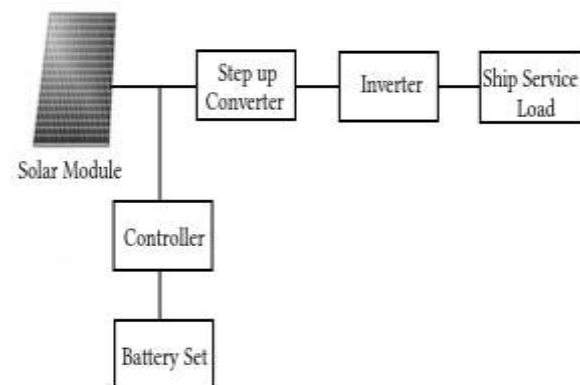


Fig. 1 Typical photovoltaic system Theoretically, the conventional step-up converters, such as the boost converter and fly-back

converters, cannot achieve a high step-up conversion and high efficiency because of the resistance of the elements or leakage inductance [2]-[4]. The answer to this problem a modified boost-fly-back converter is proposed in this paper.

As compared to the conventional circuit, losses are less in an asymmetrical interleaved converter for a high step-up and high-power application. But the asymmetrical interleaved converter circuit is complicated. One of the simplest approaches to achieve high step-up gain is by using the Modified boost-fly-back converter as shown in Fig. 2(a). Here the gain is realized by using a coupled inductor. The performance of the converter is similar to an active-clamped fly-back converter in which the leakage

energy is recovered to the output terminal [5][6]. An interleaved boost converter with a voltage-lift capacitor is shown in Fig. 2(b). It is similar to the conventional interleaved type converter. It obtains extra voltage gain through the voltage-lift capacitor, and reduces the input current ripple, which is suitable for power factor correction (PFC) and high-power applications.

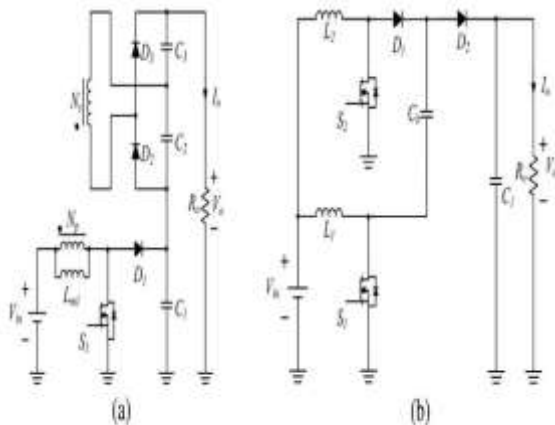


Fig. 2 (a) integrated fly-back-boost converter structure.(b) Interleaved boost converter with a voltage-lift capacitor structure.

In this paper, an asymmetrical interleaved high step-up converter is proposed with PV system having voltage multiplier module. The turns ratio of coupled inductors are designed to extend the voltage gain, and a voltage-lift capacitor is used to offer an extra voltage conversion ratio. The system designed here stores the energy in inductors and thus reduces the stress in the switches (Without allowing the total voltage to appear across the switch).

## II. OPERATING PRINCIPLE

The proposed high step-up interleaved inductor capacitor converter with voltage multiplier module is shown in Fig. 3. A boost converter with interleaved capacitor and inductor makes the system asymmetrical. Number of winding in primary is  $N_p$  and that of secondary is  $N_s$ .

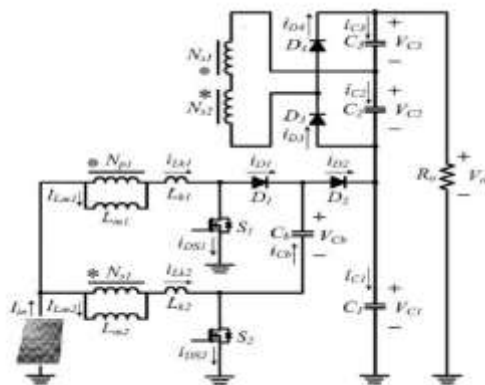


Fig. 3 The proposed converter.

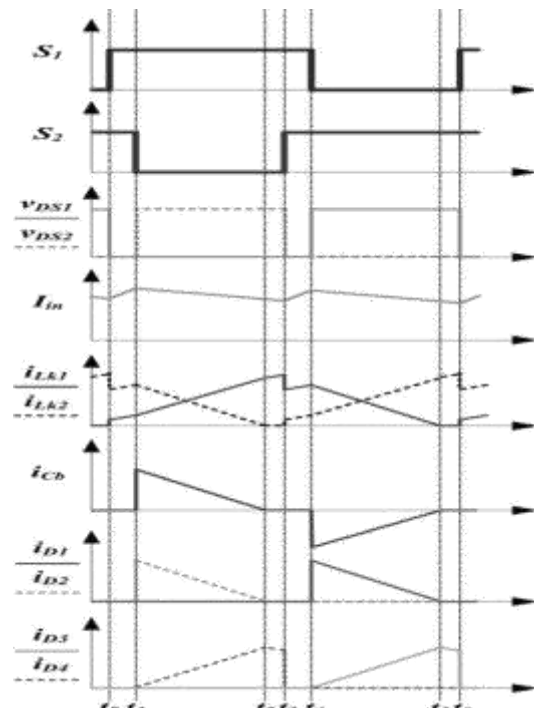


Fig. 4 Waveforms for the proposed converter .

Primary windings of the coupled inductors are employed to decrease the input current ripple, and that of secondary windings are used for extend voltage gain. The turn's ratios of the coupled

inductors are the same .In the circuit  $L_{m1}$  and  $L_{m2}$  are the magnetizing inductors,  $L_{k1}$  and  $L_{k2}$  represent the leakage inductors,  $S_1$  and  $S_2$  denote the power switches,  $C_b$  is the voltage-lift capacitor, and  $n$  is defined as a turn's ratio equal to  $N_s/N_p$ .

The proposed system operates in continuous conduction mode (CCM).The power switches during the steady state operation are interleaved with a  $180^\circ$  phase shift; the duty cycles are greater than 0.5.

The steady state waveforms in one switching period of the proposed converter have six modes, which are depicted in Fig. 4, and the different modes of operations are explained in detail in Fig. 5. In the circuit the PV system is represented by a DC voltage source.

**2.1 Mode 1 [ $t_0, t_1$ ]:** In mode 1, when  $t=t_0$  both the switches  $S_1$  and  $S_2$  are turned ON. So voltage drop across the switches  $V_{DS1}$  and  $V_{DS2}$  are zero. Diodes  $D_1$  to  $D_4$  are reverse biased. Hence capacitors are not charged. But the magnetizing inductors  $L_{m1}$  and  $L_{m2}$  as well as leakage inductors  $L_{k1}$  and  $L_{k2}$  are linearly charged by the input voltage source  $V_{in}$ . Therefore current flowing through the  $i_{Lk1}$  and  $i_{Lk2}$  starts increasing. The operation is described in fig 5 (a).

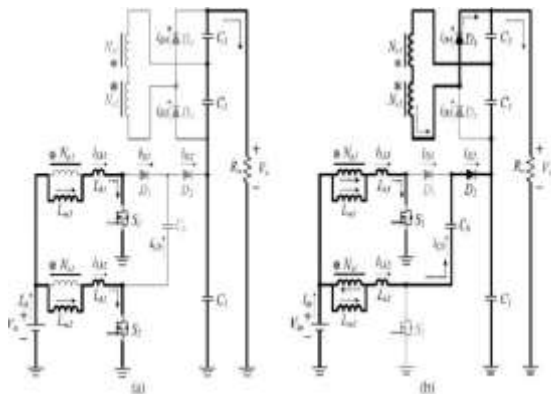


Fig.5 Operating modes (a) Mode 1 (b) Mode 2

**2.2 Mode 2** [ $t_1, t_2$ ]: When  $t=t_1$ , the power switch  $S_2$  is switched OFF, thereby diodes  $D_2$  and  $D_4$  are forward biased. The energy stored in the magnetizing inductor  $L_{m2}$  now transferred to the capacitor  $C_b$ . In this mode  $i_{Lk1}$  is increasing since the power switch  $S_1$  is on. Also  $C_2$  is charging through  $D_2$  and  $C_3$  is charging through  $D_4$ . The current flowing through the magnetizing inductor  $L_{m2}$ , leakage inductor  $L_{k2}$ , and then voltage-lift capacitor  $C_b$  releases the energy to the output capacitor  $C_1$  through the diode  $D_2$ , thereby extending the voltage on  $C_1$ .

**2.3 Mode 3** [ $t_2, t_3$ ]: At the end of  $t_2$  the capacitor  $C_b$  discharges completely and diode  $D_2$  is reverse biased automatically. Hence current through that capacitor  $i_{cb}$  is zero. In mode 3, the power switch  $S_2$  is switched OFF,  $S_1$  is ON as in the previous mode. In this mode of operation,  $C_1$  is charged completely using the energy released from the  $C_b$  through  $D_2$ . Since  $D_2$  is reverse biased capacitor  $C_2$  also discharges completely. Magnetizing inductor  $L_{m2}$  transfers energy to the secondary side charging the output filter capacitor  $C_3$  through the diode  $D_4$  until  $t_3$ .

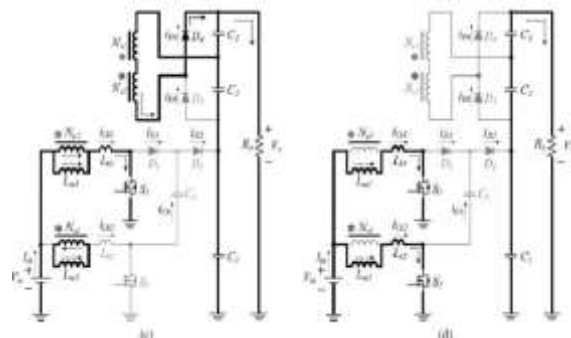


Fig 5: (c) Mode 3. (d) Mode 4

**2.4 Mode 4** [ $t_3, t_4$ ]: At time  $t=t_3$ , the power switch  $S_2$  is switched ON and all the diodes are reverse biased. The operation of mode 4 is similar to that of mode 1. Diodes  $D_1$  to  $D_4$  are reverse biased. But the magnetizing inductors  $L_{m1}$  and  $L_{m2}$  as well as leakage inductors  $L_{k1}$  and  $L_{k2}$  are linearly charged by the

input voltage source  $V_{in}$ . Fig 5 (e) and (d) explains the mode 3 and 4.

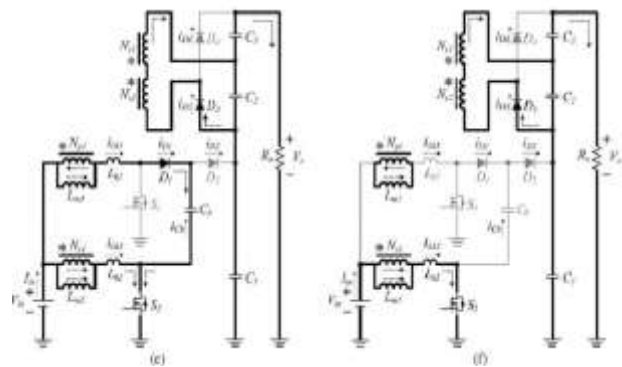


Fig 5: (e) Mode 5. (f) Mode 6

**2.5 Mode 5** [ $t_4, t_5$ ]: At  $t=t_4$ , the power switch  $S_1$  is switched OFF, which forward biases the diodes  $D_1$  and  $D_3$ .  $D_3$  is on due to the fully charged  $C_1$  capacitor. The capacitor  $C_2$  is charging from the fully charged capacitor  $C_1$ . The input voltage source and magnetizing inductor  $L_{m1}$  release energy to voltage-lift capacitor  $C_b$  through diode  $D_1$ , which stores extra energy in  $C_b$ . Since the  $C_b$  is charging through  $D_1$  the polarity is changed. Hence the  $i_{cb}$  direction is reversed.

**2.6 Mode 6** [ $t_5, t_0$ ]: At  $t=t_5$ , the diode  $D_1$  is automatically turned OFF because the total energy of leakage inductor  $L_{k1}$  has been completely released to voltage-lift capacitor  $C_b$ . Magnetizing inductor  $L_{m1}$  transfers energy to the secondary side charging the output filter capacitor  $C_2$  via diode  $D_3$  until  $t_0$ .

### III. STEADY-STATE ANALYSIS

The transient characteristics of circuitry are disregarded to simplify the circuit performance analysis of the proposed converter in CCM and some formula and assumptions are as follows:

1. All the components are ideal.
2. Leakage inductors  $L_{k1}$  and  $L_{k2}$  are neglected.
3. Voltage  $V_{Cb}, V_{C1}, V_{C2}$ , and  $V_{C3}$  are considered to be constant because of infinitely large capacitance.

#### 3.1 Voltage Gain and other voltage equations:

$$V_{Cb} = \frac{1}{1-D} V_{in} \quad (1)$$

$$V_{C1} = \frac{1}{1-D} V_{in} + V_{Cb} = \frac{2}{1-D} V_{in} \quad (2)$$

$$V_{C2} = V_{C3} = n \cdot V_{in} \left( 1 + \frac{D}{1-D} \right) = \frac{n}{1-D} V_{in} \quad (3)$$

$$V_o = V_{C1} + V_{C2} + V_{C3} = \frac{2n+2}{1-D} V_{in} \quad (4)$$

$$\frac{V_o}{V_{in}} = \frac{2n+2}{1-D} \quad (5)$$

**3.2 Voltage stresses on semiconductor components:**

$$V_{S1} = V_{S2} = \frac{1}{1-D} V_{in}. \tag{6}$$

$$V_{S1} = V_{S2} = V_o - \frac{2n+1}{1-D} V_{in}. \tag{7}$$

$$V_{D1} = V_{C1} = \frac{2}{1-D} V_{in} \tag{8}$$

$$V_{D2} = V_{C1} - V_{Cb} = \frac{1}{1-D} V_{in}. \tag{9}$$

$$V_{D1} = V_o - \frac{2n}{1-D} V_{in} \tag{10}$$

$$V_{D2} = V_o - \frac{2n+1}{1-D} V_{in}. \tag{11}$$

$$V_{D3} = V_{D4} = \frac{2n}{1-D} V_{in}. \tag{12}$$

$$V_{D3} = V_{D4} = V_o - \frac{2}{1-D} V_{in}. \tag{13}$$

**IV. SIMULATION RESULTS OF THE PROPOSED CONVERTER**

Fig 6 shows the simulation circuit of high step up converter with voltage multiplier. Simulation is done using MATLAB simulink.

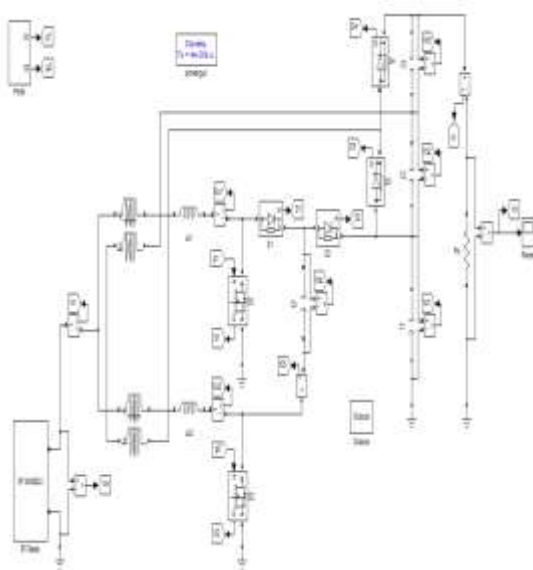


Fig 6 simulation circuit of high step-up converter with a voltage multiplier module with PV

The input voltage is taken from a PV panel and the power switches  $S_{w1}$  and  $S_{w2}$  are Power MOSFETS. The converter components used and parameter values are given in TABLE 1.

Parameters	Notations	Values
Magnetizing inductances	$L_{m1}, L_{m2}$	133 $\mu$ H
Leakage inductances	$L_{k1}, L_{k2}$	1.6 $\mu$ H
Turns ratio	$N_s/N_p$	1
Capacitors	$C_b, C_2, C_3$	220 $\mu$ F
Capacitors	$C_1$	470 $\mu$ F

TABLE 1: Converter parameters

Fig 7 shows the gate pulses  $G_1$  and  $G_2$ , voltage across the power switches  $S_{w1}$  and  $S_{w2}$ . Switch  $S_{w1}$  is ON during Mode 1 to 4. Mode 5 and 6  $S_{w1}$  is OFF. During mode 2 and 3 the switch  $S_{w2}$  is off, and in other modes it is turned ON. Fig 7 shows the gate pulses and voltage across the switches for 0.5 kW and fig 8 gives the same response for 1kW.

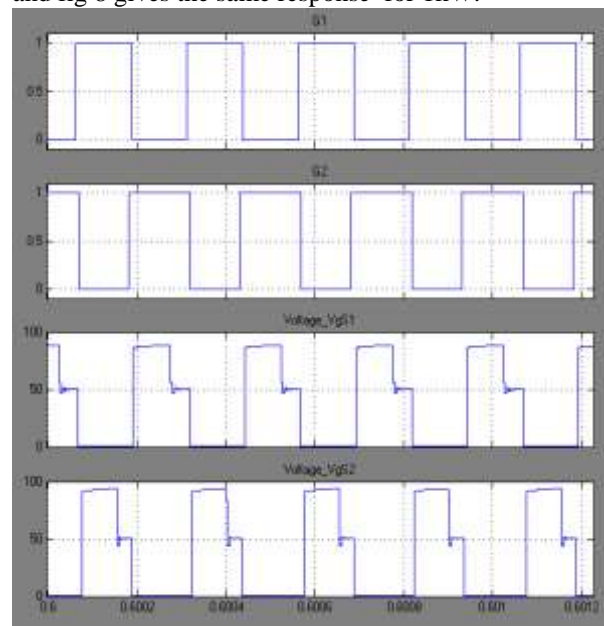


Fig 7 gate pulses & voltages across the switches  $S_{w1}$  &  $S_{w2}$  for 0.5kW power

In Fig 9 the measured input current, different leakage input current and capacitor current for 0.5kW are shown. When the switch  $S_{w1}$  is on,  $i_{Lk1}$  is increasing from zero and when  $t=t_3$  it  $i_{Lk1}$  is maximum, after that it starts to decrease and when  $t=t_5$ , current flowing through the leakage inductor  $i_{Lk1}$  again reaches zero.

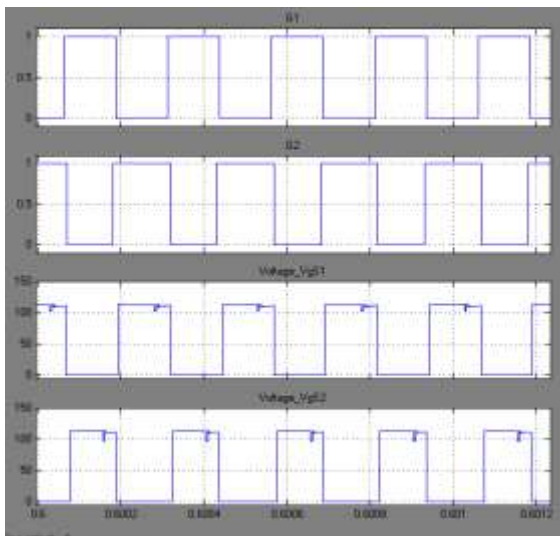


Fig 8 gate pulses & voltages across the switches  $S_{w1}$  &  $S_{w2}$  for 1kw power.

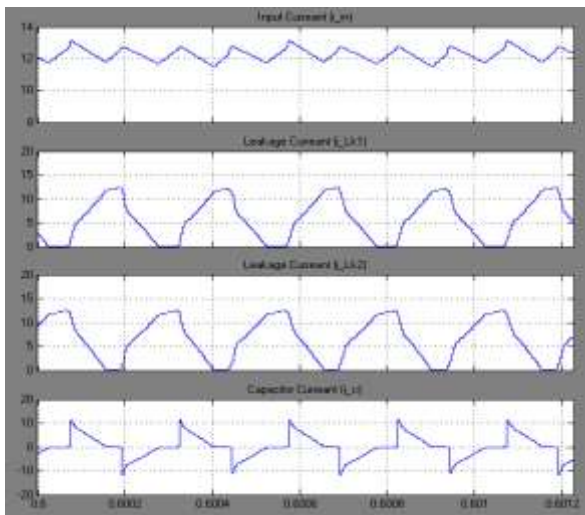


Fig 9 Measured waveforms of  $I_{in}$ ,  $I_{LK1}$ ,  $I_{LK2}$  and  $I_c$  for 0.5kw power

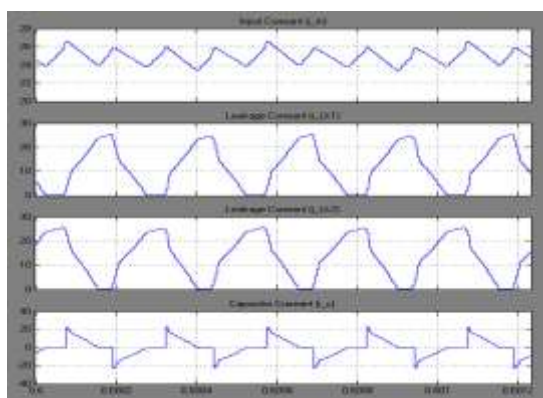


Fig 10 Measured waveforms of  $I_{in}$ ,  $I_{LK1}$ ,  $I_{LK2}$  and  $I_c$  for 1kw power

In Fig 10 leakage current and measured input current, different leakage input current and capacitor

current for 1kW. When the switch  $S_{w2}$  s on,  $i_{LK2}$  is increasing from zero and when  $t=t_0$  it  $i_{LK2}$  is maximum, after that it starts to decreases and when  $t=t_3$ , current flowing through the leakage inductor  $i_{LK2}$  again reaches zero. t.

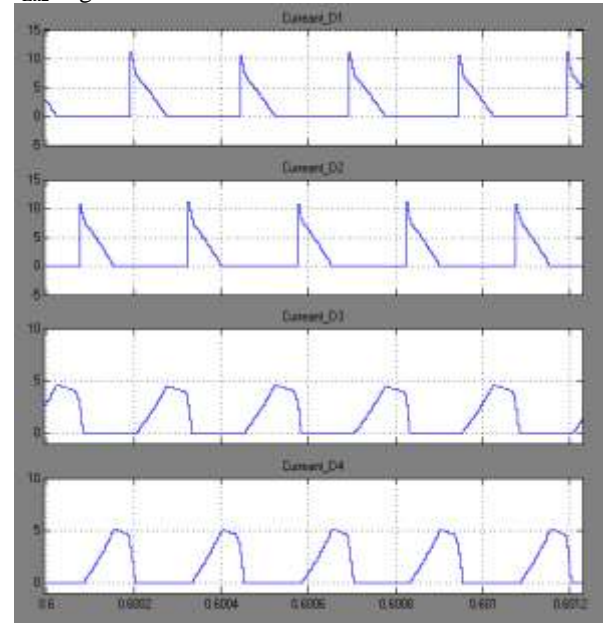


Fig 11. Measured waveforms of  $D_1$ ,  $D_2$ ,  $D_3$  and  $D_4$  for 0.5kw power

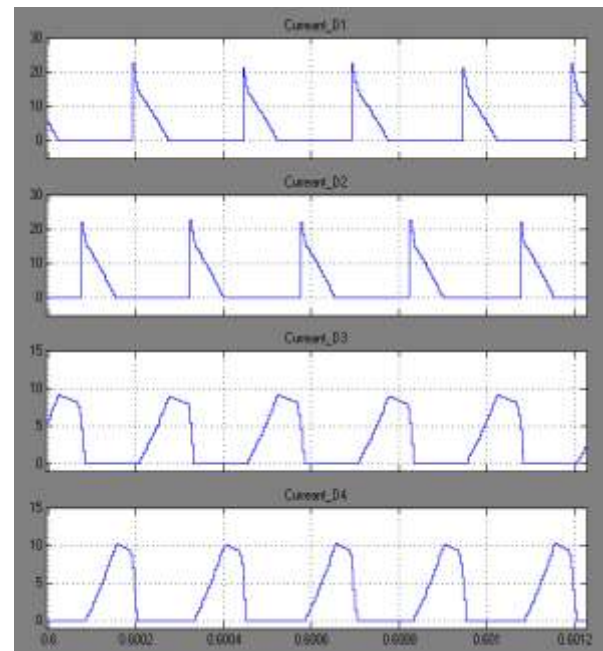


Fig 12 Measured waveforms of  $D_1$ ,  $D_2$ ,  $D_3$  and  $D_4$  for 1kw power

Fig 11 shows measured current waveforms of  $D_1, D_2, D_3, D_4$  for 0.5kW. In mode 1 all are reverse biased, hence no current flows through the circuit.

In Fig 12 it shows the different diode current at 1kW. In mode 2  $D_2, D_4$  are on where as in mode 3 and

mode 4  $D_4$  is on the rest is off. In mode 5  $D_1$  and  $D_3$  are on where as in last mode  $D_3$  is On.

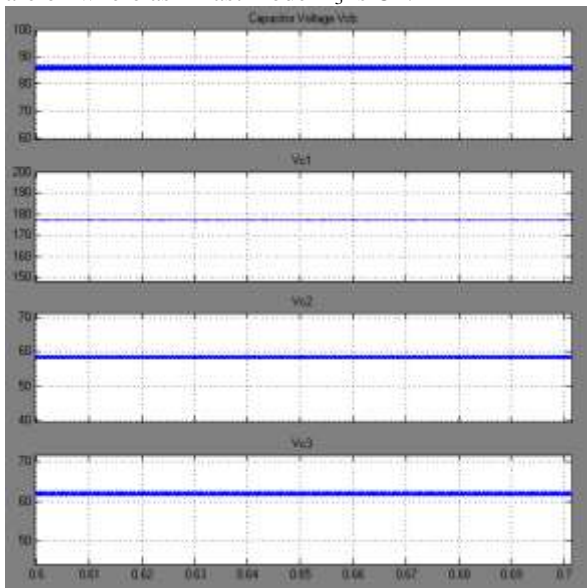


Fig 13 Waveforms of  $V_{cb}$ ,  $V_{c1}$ ,  $V_{c2}$  and  $V_{c3}$  for 0.5kw power

Fig 13 and 14 represents the voltage across different capacitors. In mode 2, each capacitor starts to charging, and  $C_b$  starts to discharge. At  $t=t_3$ ,  $C_b$  and  $C_2$  are fully discharge and again when  $t=t_4$ , capacitors  $C_2$  and  $C_b$  will again start to charge.

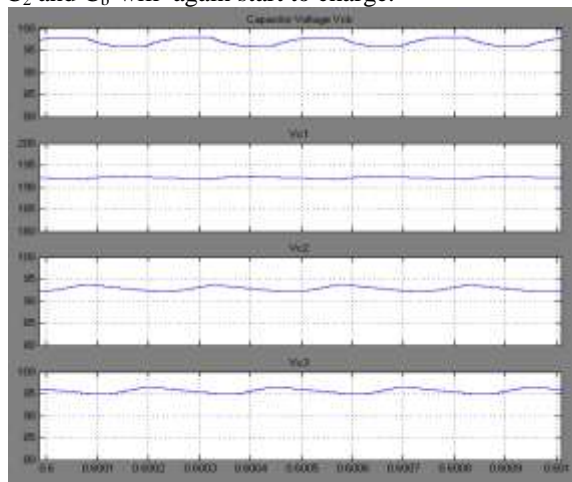


Fig 14 Waveforms of  $V_{cb}$ ,  $V_{c1}$ ,  $V_{c2}$  and  $V_{c3}$  for 1kw power

In Fig 14 gives the different capacitor current at 1kW power. Fig 15 and 16 compares the input, output power at 0.5 kW and 1kW. The voltage stress over the power switches are restricted and are much lower than the output voltage. These switches of low on-state resistance MOSFET, can be selected. The full-load efficiency at  $P_o = 1000$  W is 96.1%, and the efficiency at  $P_o = 500$  W is 96.8%.

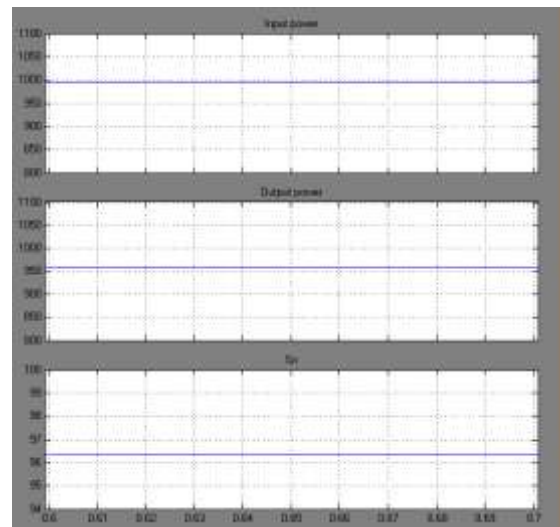


Fig 15 Waveforms of  $P_{in}$ ,  $P_o$  and  $\%n$  for 1kw power

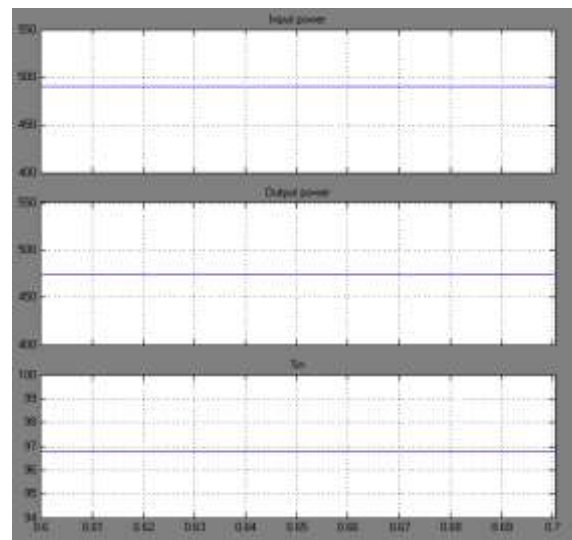


Fig 16 Waveforms of  $P_{in}$ ,  $P_o$  and  $\%n$  for 0.5kw power

## V. CONCLUSION

This paper has presented the topological principles, steady-state analysis, for a designing an efficient photovoltaic system that can be used for onboard ship applications. The converter proposed in this paper provides a efficient high step-up conversion through the voltage multiplier module and voltage clamp feature. Due to the low conduction losses and high efficiency, the proposed converter is suitable for onboard ship high power applications like blasting compressors, assault systems, radar communications etc.

## REFERENCES

### Journal Papers:

- [1] G. J. Tsekouras , F. D. Kanellos, Optimal Operation of Ship Electrical Power System with Energy Storage System and

- Photovoltaics: Analysis and Application, *WSEAS Transactions on Power Systems*, Vol 8, nno.4 Oct 2013
- [2] C. Hua, J. Lin, and C. Shen, Implementation of a DSP-controlled photovoltaic system with peak power tracking, *IEEE Trans. Ind. Electron.*, vol. 45, no. 1, 99–107, Feb. 1998
  - [3] J. M. Carrasco, L. G. Franquelo, J. T. Bialasiewicz, E. Galvan, R. C. P. Guisado, M. A.M Prats, J. I. Leon, and N. Moreno-Alfonso, Power-electronic systems for the grid integration of renewable energy sources: A survey, *IEEE Trans. Ind. Electron.*, vol. 53, no. 4, 1002– 1016, Jun. 2006.
  - [4] J. T. Bialasiewicz, Renewable energy systems with photovoltaic power generators: Operation and modeling, *IEEE Trans. Ind. Electron.*, vol. 55, no. 7, 2752–2758, Jul. 2008.
  - [5] K. Ujii, T. Izumi, T. Yokoyama, and T. Haneyoshi, Study on dynamic and static characteristics of photovoltaic cell, in *Proc. Power Convers. Conf.*, Apr. 2–5, 2002, vol. 2, 810–815.
  - [6] K. C. Tseng and T. J. Liang, Novel high-efficiency step-up converter, *IEEE Proc. Elect. Power Appl*, vol. 151, no. 2, 182–190, Mar. 2004.

**Books:**

- [7] *Future Ship Powering Options, Exploring alternative methods od ship propulsion*, Royal academy of Engineering, July 2013. R.E. Moore, Interval analysis (Englewood Cliffs, NJ: Prentice-Hall, 1966).
- [8] *Renewable Energy Options for shipping, Technological Brief*, International Renewable Energy agency, January 2015